

ITP-BUDAPEST 610
 WUB 04-05
 DESY 04-014
 hep-ph/0402102

**STRONG NEUTRINO-NUCLEON INTERACTIONS AT
 ULTRAHIGH ENERGIES AS A SOLUTION TO THE GZK PUZZLE***

Z. FODOR^{1,2}, S. D. KATZ^{2†}, A. RINGWALD³ AND H. TU³

¹*Institute for Theoretical Physics,
 Eötvös University,
 H-1518 Budapest, Pf. 32, Hungary*

²*Department of Physics,
 University of Wuppertal,
 D-42097 Wuppertal, Germany*

³*Deutsches Elektronen-Synchrotron DESY,
 D-22603 Hamburg, Germany*

After a short review of the ultrahigh energy cosmic ray puzzle – the apparent observation of cosmic rays originating from cosmological distances with energies above the expected Greisen-Zatsepin-Kuzmin cutoff 4×10^{19} eV – we consider strongly interacting neutrino scenarios as an especially interesting solution. We show that all features of the ultrahigh energy cosmic ray spectrum from 10^{17} eV to 10^{21} eV can be described to originate from a simple power-like injection spectrum of protons, under the assumption that the neutrino-nucleon cross-section is significantly enhanced at center of mass energies above ≈ 100 TeV. In such a scenario, the cosmogenic neutrinos produced during the propagation of protons through the cosmic microwave background initiate air showers in the atmosphere, just as the protons. The total air shower spectrum induced by protons and neutrinos shows excellent agreement with the observations. We shortly discuss TeV-scale extensions of the Standard Model which may lead to a realization of a strongly interacting neutrino scenario. We emphasize, however, that such a scenario may even be realized within the standard electroweak model: electroweak instanton/sphaleron induced processes may get strong at ultrahigh energies. Possible tests of strongly interacting neutrino scenarios range from observations at cosmic ray facilities and neutrino telescopes to searches at lepton nucleon scattering experiments.

1. Introduction

The Earth's atmosphere is continuously bombarded by cosmic particles (“rays”). Their measured flux extends over many orders of magnitude in energy (cf. Fig. 1). At energies above 10^{15} eV, they are observed in the form of extensive air showers (EAS's), initiated by inelastic scattering processes of cosmic particles off atmospheric nucleons. Ground-based observatories have measured EAS's with en-

*Invited talk given at the 10th Marcel Großmann Meeting, 20-26 July 2003, Rio de Janeiro, Brazil.

†On leave from Institute for Theoretical Physics, Eötvös University, Budapest, Hungary.

ergies up to $E \lesssim 3 \times 10^{20}$ eV, corresponding to center-of-mass (CM) energies $\sqrt{s} = \sqrt{2m_p E} \lesssim 750$ TeV, where m_p is the proton mass. Therefore, the highest energy cosmic rays probe physics beyond the reach of the (Very³) Large Hadron Collider⁴ ((V)LHC), with a projected CM energy of 14 (200) TeV. In this context, it is interesting that the measured cosmic ray flux at the highest energies, $E \gtrsim 10^{20}$ eV, represents a puzzle. What is this puzzle about?

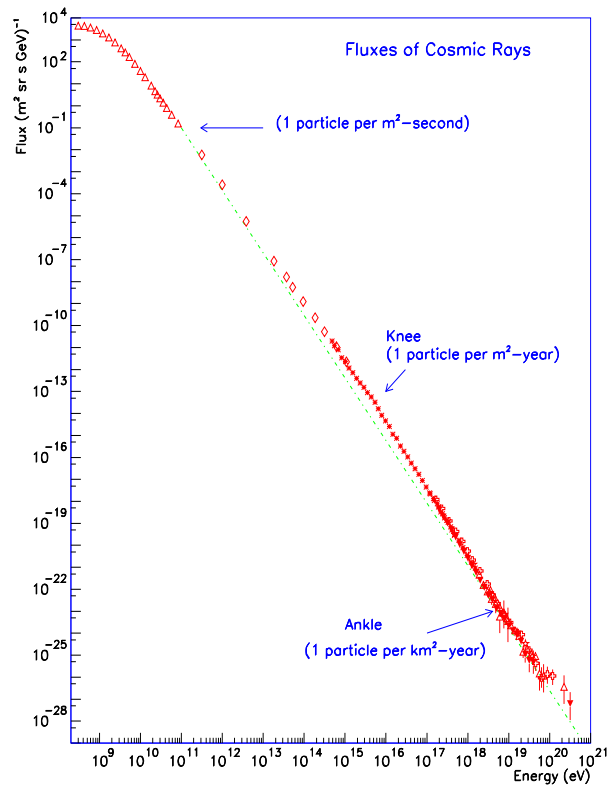


Figure 1. Compilation of measurements of the flux of cosmic rays. The dotted line shows an E^{-3} power-law for comparison. Approximate integral fluxes (per steradian) are also shown (adapted¹ from Ref.²).

It hinges on the circumstantial evidence that the cosmic rays above $10^{17.5 \div 18.5}$ eV originate from cosmological distances (for a recent review, see Ref.⁵). This evidence is largely based on the apparent large-scale isotropy in the arrival directions of cosmic rays (cf. Fig. 2). Moreover, whereas there are only very few – if any – nearby source candidates, plausible astrophysical sources are most likely to be found only at cosmological distances.

If the highest energy cosmic rays are nucleons (or nuclei), if their sources are

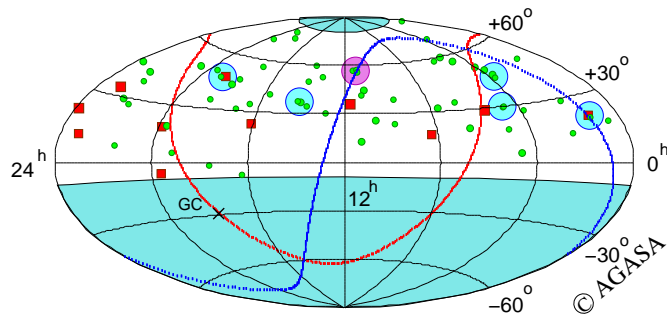


Figure 2. Arrival directions of cosmic rays detected by the AGASA and Akeno (A20) experiments in equatorial coordinates. Open circles and open squares represent cosmic rays with energies $(4 \div 10) \times 10^{19}$ eV, and $\geq 10^{20}$ eV, respectively. The galactic and super-galactic planes are shown by the red and blue curves, respectively. Large shaded circles indicate event clusters within 2.5° . The shaded regions indicate the celestial regions excluded by a zenith angle cut of $\leq 45^\circ$. Update⁶ (June 24, 2003) of the published data from Ref.⁷.

indeed uniformly distributed at cosmological distances, and if their injection spectra are power-laws in energy – a reasonable assumption, in view of the measured spectrum in Fig. 1 which appears to be approximately of (broken) power-law type over many order of magnitude in energy – then their total flux arriving at Earth should show a pronounced drop above the Greisen-Zatsepin-Kuzmin⁸ (GZK) “cut-off” $E_{\text{GZK}} = 4 \times 10^{19}$ eV. This is due to the fact that, above this energy, the universe becomes opaque to high energy nucleons (and nuclei), due to inelastic hadronic scattering processes with the cosmic microwave background (CMB) photons. The GZK cutoff is, however, not seen in the data, at least not in a significant manner (cf. Fig. 3). Correspondingly, the events above 10^{20} eV in Fig. 3 should originate from small distances below 50 Mpc, the typical interaction length of nucleons above E_{GZK} . However, no source within a distance of 50 Mpc is known in the arrival directions of the post-GZK events^a. The basic puzzle is: if the sources of ultrahigh energy cosmic rays are indeed at cosmological distances, how could they reach us with energies above 10^{20} eV?

At the relevant energies, among the known particles only neutrinos can propagate without significant energy loss from cosmological distances to us. It is this fact which led, on the one hand, to scenarios invoking hypothetical – beyond the Standard Model – strong interactions of ultrahigh energy cosmic neutrinos¹⁸ and, on the other hand, to the Z-burst scenario^{19,20}.

In the latter, ultrahigh energy cosmic neutrinos (UHEC ν 's) produce Z-bosons through annihilation with the relic neutrino background from the big bang. On

^aThe dominant radio galaxy M87 in the Virgo cluster, at a distance of about 20 Mpc, has been a source candidate for a long time¹⁴. The major difficulty with this idea is the isotropy of the arrival distribution. It might be overcome by invoking a particular galactic magnetic field originating from a “galactic wind”¹⁵. Criticisms of this model¹⁶ have been addressed in Ref.¹⁷.

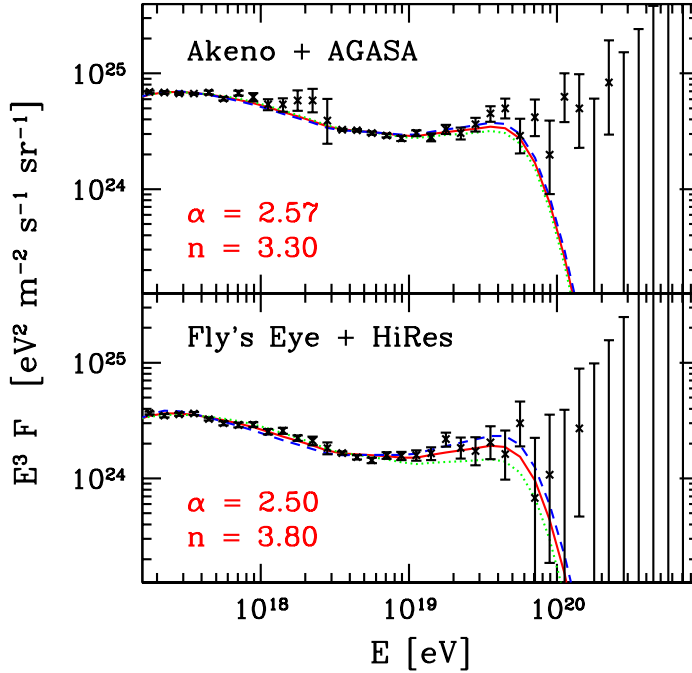


Figure 3. Ultrahigh energy cosmic ray data with their statistical errors (top: combination of Akeno⁹ and AGASA¹⁰ data; bottom: combination of Fly's Eye¹¹ and HiRes¹² data) and the predictions arising from a power-law emissivity distribution (1) corresponding to sources which are uniformly distributed at cosmological distances. The best fits between $E_- = 10^{17.2}$ eV and $E_+ = 10^{20}$ eV are given by the solid lines and correspond to the indicated values of the parameters α and n in the source emissivity distribution. The 2-sigma variations corresponding to the minimal (dotted) and maximal (dashed) fluxes are also shown. Other parameters of the analysis were $E_{\max} = 3 \times 10^{21}$ eV, $z_{\min} = 0.012$, and $z_{\max} = 2$. From Ref.¹³.

Earth, we observe the air showers initiated by the protons and photons from the hadronic decays of these Z-bosons. Though the required ultrahigh energy cosmic neutrino flux²⁰ is smaller than present upper bounds²¹, it is not easy to conceive a production mechanism yielding a sufficiently large one. In the near future, UHEC ν detectors, such as the Pierre Auger Observatory²², IceCube²³, ANITA²⁴, EUSO²⁵, OWL²⁶, and SalSA²⁷ can directly confirm or exclude this scenario²⁸.

Scenarios based on strongly interacting neutrinos, on the other hand, are based on the observation that the flux of neutrinos originating from the decay of the pions produced during the propagation of nucleons through the CMB^{18,29,30,31} – the cosmogenic neutrinos – shows a nice agreement with the observed ultrahigh energy cosmic ray (UHECR) flux above E_{GZK} . Assuming a large enough neutrino-nucleon cross-section at these high energies, these neutrinos could initiate extensive air showers high up in the atmosphere, like hadrons, and explain the existence of the post-GZK events¹⁸. This large cross-section is usually ensured by new types of TeV-scale interactions beyond the Standard Model, such as arising through gluonic

bound state leptons³², through TeV-scale grand unification with leptoquarks³³, through Kaluza-Klein modes from compactified extra dimensions³⁴ (see, however, Ref.³⁵), or through p -brane production in models with warped extra dimensions³⁶ (see, however, Ref.³⁷); for earlier and further proposals, see Ref.³⁸ and Ref.³⁹, respectively.

In this review, we discuss strongly interacting neutrino scenarios as a possible solution to the GZK puzzle. We present a detailed statistical analysis of the agreement between observations and predictions from such scenarios⁴⁰. Moreover, we emphasize an example which – in contrast to previous proposals – is based entirely on the Standard Model of particle physics. It exploits non-perturbative electroweak instanton-induced processes for the interaction of cosmogenic neutrinos with nucleons in the atmosphere, which may have a sizeable cross-section above a threshold energy $E_{\text{th}} = \mathcal{O}((4\pi m_W/\alpha_W)^2)/(2m_p) = \mathcal{O}(10^{18})$ eV, where m_W denotes the W-boson mass and α_W the electroweak fine structure constant^{41,42,43}.

Our scenario is based on a standard power-like primary spectrum of protons injected from sources at cosmological distances. After propagation through the CMB, these protons will have energies below E_{GZK} , so they can well describe the low energy part of the UHECR spectrum. The cosmogenic neutrinos interact with the atmosphere and thus give a second component to the UHECR flux, which describes the high energy part of the spectrum. The relative normalization of the proton and neutrino fluxes is fixed in this scenario, so the low and high energy parts of the spectrum are explained simultaneously without any extra normalization. Details of this analysis can be found in Ref.⁴⁰.

The structure of this review is as follows. In the next section, we review our procedure to infer the fluxes of protons and cosmogenic neutrinos at Earth, from an assumed injection spectrum at the sources. In Sect. 3, various possibilities, including the one exploiting electroweak instantons, for a large neutrino-nucleon cross-section at high energies are discussed, and the induced air shower rate is calculated. In Sect. 4, we present a comparison of the predictions with the observations and a determination of the goodness of the fit. Possible further tests are mentioned in Sect. 5, while conclusions are given in Sect. 6.

2. Proton and cosmogenic neutrino fluxes

Our analysis⁴⁰ is based on the assumption of a power-law emissivity distribution corresponding to uniformly distributed sources. The emissivity is defined as the number of protons per co-moving volume per unit of time and per unit of energy, injected into the CMB with energy E_i and characterized by a spectral index α and a redshift (z) evolution index n ,

$$\mathcal{L}_p = j_0 E_i^{-\alpha} (1+z)^n \theta(E_{\text{max}} - E_i) \theta(z - z_{\text{min}}) \theta(z_{\text{max}} - z). \quad (1)$$

Here, j_0 is a normalization factor, which will be fixed by the observed flux. The parameters E_{max} and $z_{\text{min}/\text{max}}$ have been introduced to take into account certain

possibilities such as the existence of a maximal energy, which can be reached through astrophysical accelerating processes in a bottom-up scenario, and the absence of nearby/very early sources, respectively. Our predictions are quite insensitive to the specific choice for E_{\max} , z_{\min} , and z_{\max} , within their anticipated values. The main sensitivity arises from the spectral parameters α and n , for which we determine the 1- and 2-sigma confidence regions in Sect. 4.

The propagation of particles can be described^{30,44,45} by $P_{b|a}(z, E_i; E)$ functions, which give the expected number of particles of type b above the threshold energy E if one particle of type a started at a redshift “distance” z with energy E_i . With the help of these propagation functions, the differential flux of protons ($b = p$) and cosmogenic neutrinos ($b = \nu_i, \bar{\nu}_i$) at Earth can be written as

$$F_b(E) = \frac{1}{4\pi} \int_0^\infty dE_i \int_0^\infty \frac{dz}{H(z)} \frac{-\partial P_{b|p}(z, E_i; E)}{\partial E} \frac{\mathcal{L}_p(r, E_i)}{1+z}. \quad (2)$$

In our analysis, we took $z_{\max} = 2$ (cf. Ref. ⁴⁶), while we choose $z_{\min} = 0.012$ in order to take into account the fact that within 50 Mpc there are apparently no astrophysical sources of UHECR’s. We used the expression $H^2(z) = H_0^2 [\Omega_M (1+z)^3 + \Omega_\Lambda]$ for the relation of the Hubble expansion rate at redshift z to the present one. Un-

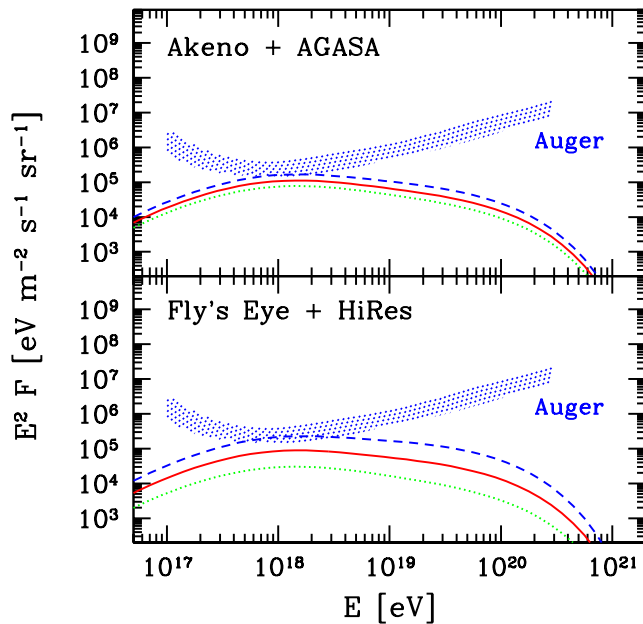


Figure 4. Predicted cosmogenic neutrino fluxes per flavor, $F_{\nu_\ell} + F_{\bar{\nu}_\ell}$, $\ell = e, \mu, \tau$, originating from a power-law proton source emissivity distribution (1) and corresponding to the predicted UHECR fluxes in Fig. 3. The “best” predictions for the neutrino spectra are given by the solid lines. The 2-sigma variations corresponding to the minimal (dotted) and maximal (dashed) fluxes are also shown. The dotted band labelled by Auger represents the expected sensitivity of the Pierre Auger Observatory to $\nu_\tau + \bar{\nu}_\tau$, corresponding to one event per year per energy decade⁵⁰. From Ref.¹³.

certainties of the latter, $H_0 = h$ 100 km/s/Mpc, with⁴⁷ $h = (0.71 \pm 0.07) \times 0.95^{1.15}$, are included. Ω_M and Ω_Λ , with $\Omega_M + \Omega_\Lambda = 1$, are the present matter and vacuum energy densities in terms of the critical density. As default values we choose $\Omega_M = 0.3$ and $\Omega_\Lambda = 0.7$, as favored today. Our results turn out to be rather insensitive to the precise values of the cosmological parameters.

We calculated $P_{b|a}(z, E_i; E)$ in two steps. *i)* First, the SOPHIA Monte-Carlo program⁴⁸ was used for the simulation of photohadronic processes of protons with the CMB photons. For e^+e^- pair production, we used the continuous energy loss approximation, since the inelasticity is very small ($\approx 10^{-3}$). We calculated the $P_{b|a}$ functions for “infinitesimal” steps as a function of the redshift z . *ii)* We multiplied the corresponding infinitesimal probabilities starting at a redshift z down to Earth with $z = 0$. The details of the calculation of the $P_{b|a}(z, E_i; E)$ functions for protons, neutrinos, charged leptons, and photons will be published elsewhere⁴⁹.

Since the propagation functions are of universal usage, we decided to make the latest versions of $-\partial P_{b|a}/\partial E$ available for the public via the World-Wide-Web URL www.desy.de/~uhecr.

As an illustration of the outcome of our propagation codes, we display in Fig. 3 the predictions for the proton flux at Earth, originating from a power-like source emissivity distribution (1) with particular α, n, \dots values indicated on the figure and in its caption. A nice fit of the data can be obtained apparently for energies below $\lesssim 4 \times 10^{19}$ eV = E_{GZK} – more on this in Sect. 4. The associated predicted cosmogenic neutrino flux, for the same parameter values, is displayed in Fig. 4.

3. Spectrum of neutrino-induced air showers

The main assumption of strongly interacting neutrino scenarios is that the neutrino-nucleon cross-section $\sigma_{\nu N}^{\text{tot}}$ suddenly becomes much larger than ≈ 1 mb above center of mass energies $\sqrt{s} \approx 100$ TeV. In this case, the corresponding neutrino interaction length $\lambda_\nu \equiv m_p/\sigma_{\nu N}^{\text{tot}}$, with $\sigma_{\nu N}^{\text{tot}} = \sigma_{\nu N}^{\text{cc}} + \sigma_{\nu N}^{\text{new}}$, falls below $X_0 = 1031$ g/cm² – the vertical depth of the atmosphere at sea level – above the neutrino threshold energy $\approx 10^{19}$ eV. Here $\sigma_{\nu N}^{\text{cc}}$ and $\sigma_{\nu N}^{\text{new}}$ denote the charged current and the new contribution to the cross-section. Above the neutrino threshold energy, the atmosphere becomes opaque to cosmogenic neutrinos and most of them will end up as air showers. Quantitatively, this fact can be described by

$$F'_\nu(E) = F_\nu(E) \left[1 - e^{-\frac{X(\theta)}{\lambda_\nu(E)}} \right] = F_\nu(E) \times \begin{cases} \frac{X(\theta)}{\lambda_\nu(E)} & \text{for } \lambda_\nu(E) \gg X(\theta) \\ 1 & \text{for } \lambda_\nu(E) \ll X(\theta) \end{cases}, \quad (3)$$

which gives the spectrum of neutrino-initiated air showers, for an incident cosmogenic neutrino flux $F_\nu = \sum_i [F_{\nu_i} + F_{\bar{\nu}_i}]$ from Eq. (2), in terms of the atmospheric depth $X(\theta)$, with θ being the zenith angle.

Such suddenly increasing cross-sections have been proposed in various models involving physics beyond the Standard Model^{32,33,34,35,36,37,38,39}. Among

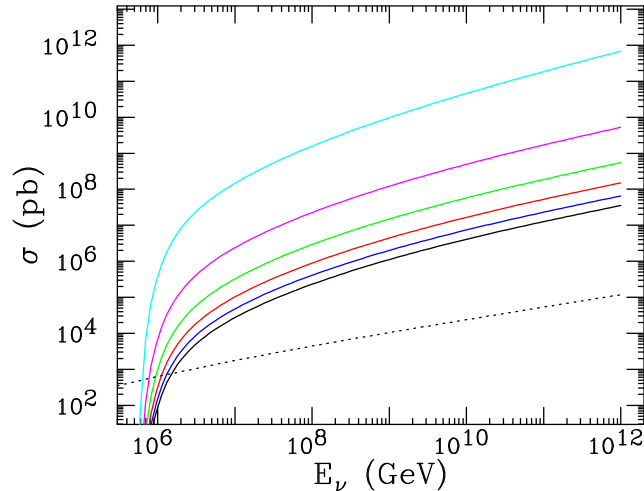


Figure 5. Total cross section $\sigma(\nu N \rightarrow p\text{-brane})$ in a model with $n = 6$ extra dimensions, out of which m have a size $L/L_* = 0.25$ in terms of the fundamental Planck length $L_* = M_*^{-1}$, for $m = 0, \dots, n-1$ from below. The fundamental Planck scale $M_D = [(2\pi)^n/8\pi]^{1/(n+2)} M_*$ has been chosen as $M_D = M_p^{\text{min}} = 1$ TeV in terms of the minimum p -brane mass M_p^{min} . The Standard Model charged current cross-section $\sigma(\nu N \rightarrow \ell X)$ is also shown (dotted). From Ref.³⁷.

the usual suspects are TeV-scale gravity scenarios with large or warped extra dimensions⁵¹. In those, the neutrino-nucleon cross-section may be greatly enhanced compared to the Standard Model one. As an example, we demonstrate in Fig. 5 that p -brane production in neutrino-nucleon scattering^{36,37} may reach a cross-section of ≈ 10 mb at $\approx 10^{19}$ eV, depending on the parameters of the model. This is in contrast to microscopic black hole ($\equiv 0$ -brane) production⁵² which has generically too small a cross-section⁵³ to solve the GZK puzzle, within the allowed parameter ranges.

In Fig. 6, we show another example for a strong enhancement in the neutrino-nucleon cross-section, which is based entirely on the Standard Model, exploiting non-perturbative electroweak instanton-induced processes^{41,42,43}. According to the estimates presented in Fig. 6, the electroweak instanton-induced neutrino-nucleon cross-section appears to have a threshold-like behavior at $E_{\text{th}} = \mathcal{O}((4\pi m_W/\alpha_W)^2)/(2m_p) = \mathcal{O}(10^{18})$ eV, above which it quickly rises above 1 mb. Our quantitative analysis in Ref.⁴⁰ was based on the cross-section from Ref.⁴³ (solid line in Fig. 6), however it is quite insensitive to the exact form of it as long as it rises abruptly far above 1 mb. Note that such a behaviour is consistent with present upper bounds on electroweak instanton-induced cross-sections^{56,57}. However, it is fair to say that there are substantial uncertainties in the predictions in Fig. 6: the absolute size of the cross-section above the threshold energy may well be unobservably small.

4. Comparison with UHECR data

The predicted air shower rate induced by protons and neutrinos is given by

$$F_{\text{pred}}(E; \alpha, n, E_{\text{max}}, z_{\text{min}}, z_{\text{max}}, j_0) = F_p(E; \dots) + F'_\nu(E; \dots). \quad (4)$$

In Ref.⁴⁰, we performed a statistical analysis to compare the prediction (4), within the electroweak instanton scenario from Fig. 6 (solid), with the observations and presented a measure for the goodness of the scenario. We gave the best fit to the observations and the 1- and 2-sigma confidence regions in the (α, n) plane.

To start the analysis, we had to convert the measured fluxes, which UHECR collaborations usually publish in a binned form, into event numbers in each bin. We used the most recent results of the HiRes and AGASA collaborations and did our analysis separately with both data sets. We concentrated on the energy range $10^{17.2} \text{ eV} - 10^{21} \text{ eV}$ which is divided into 38 equal logarithmic bins. In the low energy region, there are no published results available from AGASA and only low statistics results from HiRes-2. Therefore, we included the results of the predecessor collaborations – Akeno⁹ and Fly’s Eye, respectively – into the analysis. With a small normalization correction, it was possible to continuously connect the AGASA data¹⁰ with the Akeno ones and the HiRes-1 monocular data¹² with the Fly’s Eye stereo ones¹¹, respectively (cf. Figs. 3 and 7).

The goodness of the scenario was determined by a statistical analysis. We determined the compatibility of different (α, n) pairs (cf. Eqs. (1) and (4)) with the experimental data. For some fixed (α, n) pair, the expected number of events in individual bins are $(\lambda = \{\lambda_1, \dots, \lambda_r\})$ with r being the total number of bins (in our

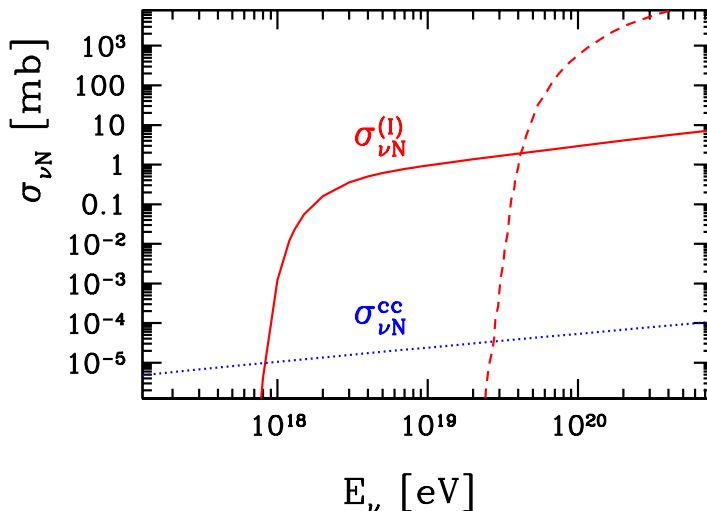


Figure 6. Predictions of the electroweak instanton-induced neutrino-nucleon cross-section $\sigma_{\nu N}^{(I)}$ (solid⁴⁰ and dashed⁵⁴) in comparison with the charged current cross-section $\sigma_{\nu N}^{\text{cc}}$ (dotted) from Ref.⁵⁵, as a function of the neutrino energy E_ν in the nucleon’s rest frame.

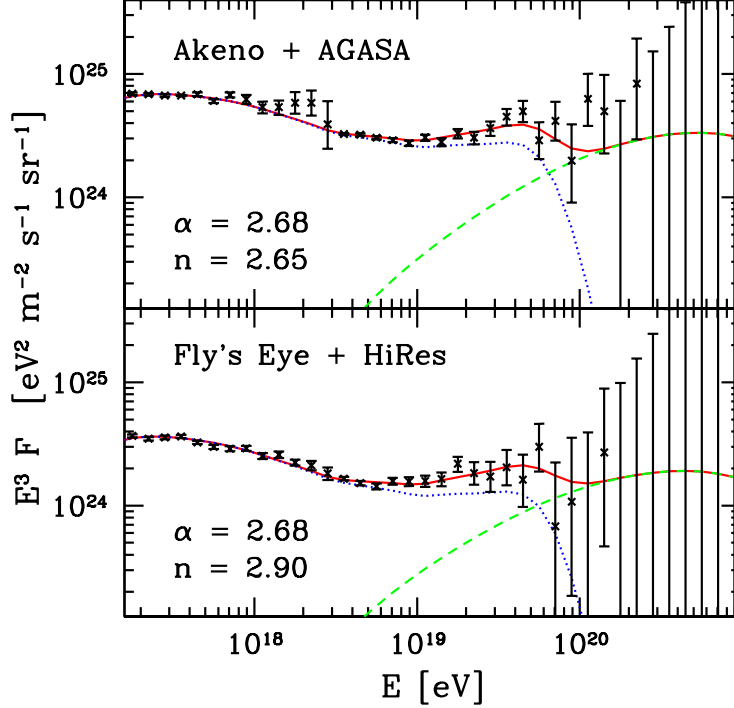


Figure 7. Ultrahigh energy cosmic ray data (Akeno + AGASA on the upper panel and Fly’s Eye + HiRes on the lower panel) and their best fits (solid) within the electroweak instanton scenario from Fig. 6 (solid) for $E_{\max} = 3 \times 10^{22}$ eV, $z_{\min} = 0.012$, $z_{\max} = 2$, consisting of a proton component (dotted) plus a cosmogenic neutrino-initiated component (dashed). From Ref.⁴⁰.

case 38). The probability of getting an experimental outcome $\mathbf{k} = \{k_1, \dots, k_r\}$ (where k_i are non-negative integer numbers) is given by the probability distribution function $P(\mathbf{k})$, which is just the product of Poisson distributions for the individual bins. We also included the $\approx 30\%$ overall energy uncertainty into the $P(\mathbf{k})$ probability distribution. We denote the experimental result by $\mathbf{s} = \{s_1, \dots, s_r\}$, where the s_i -s are non-negative, integer numbers. The (α, n) pair is compatible with the experimental results if

$$\sum_{\mathbf{k} | P(\mathbf{k}) > P(\mathbf{s})} P(\mathbf{k}) < c. \quad (5)$$

For a 1-(or 2)-sigma compatibility one takes $c=0.68$ (or $c=0.95$), respectively. The best fit is found by minimizing the sum on the left hand side.

Figure 7 shows our best fits for the AGASA and for the HiRes UHECR data. The best fit values are $\alpha = 2.68(2.68)$ and $n = 2.65(2.9)$, for AGASA(HiRes), within the electroweak instanton scenario from Fig. 6 (solid). We can see very nice agreement with the data within an energy range of nearly four orders of magnitude. The fits are insensitive to the value of E_{\max} as far as we choose a value above $\approx 3 \times 10^{21}$ eV.

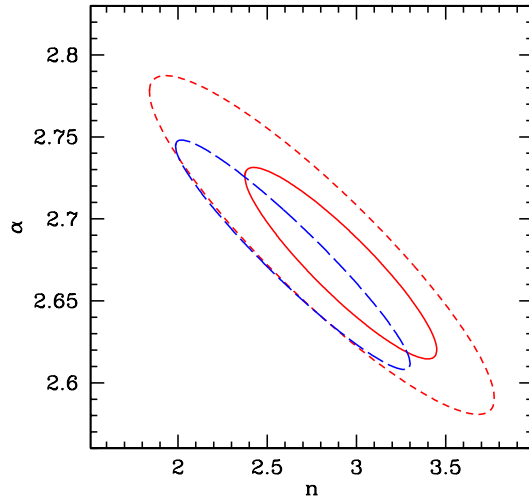


Figure 8. Confidence regions in the α - n plane for fits to the Akeno + AGASA data (2-sigma (long dashed)) and to the Fly's Eye + HiRes data (1-sigma (solid); 2-sigma (short-dashed)), respectively, within the electroweak instanton scenario from Fig. 6 (solid), for $E_{\max} \gtrsim 3 \times 10^{21}$ eV, $z_{\min} \geq 0$, $z_{\max} = 2$. From Ref.⁴⁰.

The shape of the curve between 10^{17} eV and 10^{19} eV is mainly determined by the redshift evolution index n . At these energies the universe is already transparent for protons created at $z \approx 0$, while protons from sources with larger redshift accumulate in this region. The more particles are created at large distances – i.e. the larger n is – the stronger this accumulation should be. In this context, we note that the data seem to confirm our implicit assumption that the extragalactic uniform UHECR component begins to dominate over the galactic one already at $\approx 10^{17}$ eV. If we, alternatively, start our fit only at $10^{18.5}$ eV – corresponding to the assumption that the galactic component dominates up to this energy – we find, however, also a very good fit, with a very mild dependence on n and the same best fit values for α , with a bit larger uncertainties. The peak around 4×10^{19} eV in Fig. 7 shows the accumulation of particles due to the GZK effect. Neutrinos start to dominate over protons at around 10^{20} eV.

It is important to note that, if we omit the neutrino component, then the model is ruled out on the 3-sigma level for both experiments. This is due to the fact that we excluded nearby sources by setting $z_{\min} \neq 0$ (see also Ref.⁵⁸). The choice $z_{\min} = 0$ makes the HiRes data compatible with a proton-only scenario on the 2-sigma level (see also Refs.^{12,59}).

Figure 8 displays the confidence regions in the (α, n) plane for AGASA and HiRes. The scenario is consistent on the 2-sigma level with both experiments. For HiRes, the compatibility is even true on the 1-sigma level. It is important to note that both experiments favor the same values for α and n , demonstrating their mutual compatibility on the 2-sigma level (see also Ref.⁶⁰). If we ignore the energy

uncertainty in the determination of the goodness of the fit, they turn out to be inconsistent.

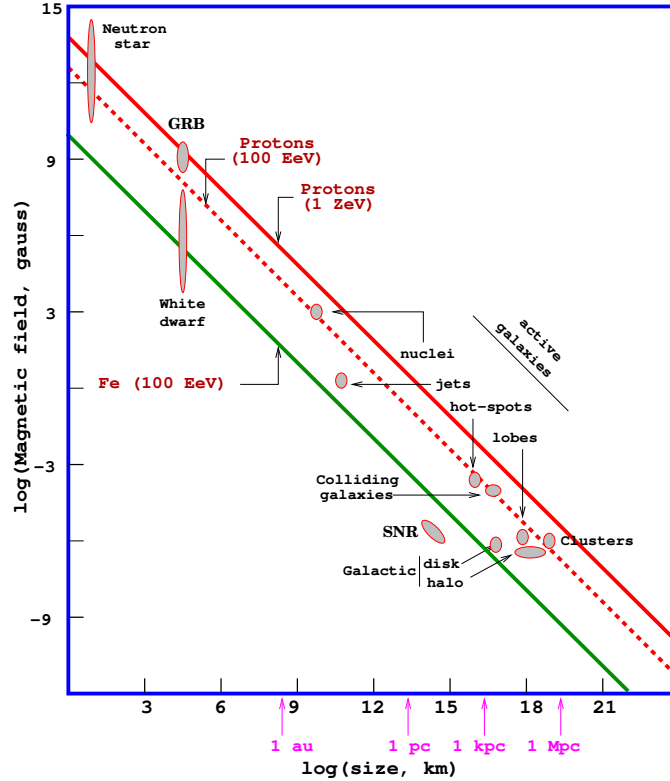


Figure 9. The Hillas diagram showing size and magnetic field strengths of possible sites of particle acceleration. Objects below the diagonal lines (from top to bottom), derived from the Hillas criterion⁶¹ $E_{\max} \sim 2ZeBr$ for the maximum energy acquired by a particle of charge Ze traveling in a medium of size r with a magnetic field B , cannot shock accelerate protons above 10^{21} eV, above 10^{20} eV and iron nuclei above 10^{20} eV, respectively. (This version of the picture is courtesy of Murat Boratav).

Finally, let us emphasize that the same fit results are valid for all strongly interacting neutrino scenarios, as long as the neutrino-nucleon cross-section has a similar threshold-like behavior as in Figs. 5 and 6, with a neutrino threshold energy $\lesssim 4 \times 10^{19}$ eV and a cross-section $\gtrsim 1$ mb above threshold. It is also important to note that the energy requirements on the sources of the primary protons are comparatively mild. To obtain a good fit, we need $E_{\max} \gtrsim 3 \times 10^{21}$ eV. An inspection of the Hillas diagram in Fig. 9 reveals that there are a number of reasonable astrophysical source candidates, notably neutron stars and gamma ray bursters (GRB's), which may provide the necessary conditions to accelerate protons to the required energies by conventional shock acceleration.

5. Further tests

There are a number of further possible tests of strongly interacting neutrino scenarios, ranging from astroparticle tests, which include searches at EAS arrays and neutrinos telescopes, to laboratory tests at present and future accelerators. We will review some of those in this Section.

5.1. Astroparticle tests

5.1.1. Searches at EAS arrays

One possibility to test the ultrahigh energy neutrino component in the EAS data is to study the zenith angle dependence of the events in the $10^{18\div 20}$ eV range, which will reflect the energy dependence of the neutrino-nucleon cross-section^{42,62}. Near the threshold energy in strongly interacting neutrino scenarios, there will be always a range of energies where the cross-section is already sizable, but does not yet reach hadronic values (cf. Figs. 5 and 6), in particular, where $\sigma_{\nu N}^{\text{tot}} \lesssim 0.56$ mb, corresponding to the atmospheric depth at larger zenith angles, $\theta \gtrsim 70^\circ$. Therefore, for these energies, neutrino-initiated showers can be searched for at cosmic ray facilities by looking for quasi-horizontal air showers⁴², $\theta \gtrsim 70^\circ$. We have checked in Ref.⁴⁰ that the rate from our electroweak instanton prediction (cf. Fig. 6) is consistent with observational constraints found by the Fly's Eye⁶³ and AGASA⁶⁴ collaborations. For the case of p -brane production, such constraints can be avoided in warped extra dimension scenarios with fine-tuned sizes³⁷.

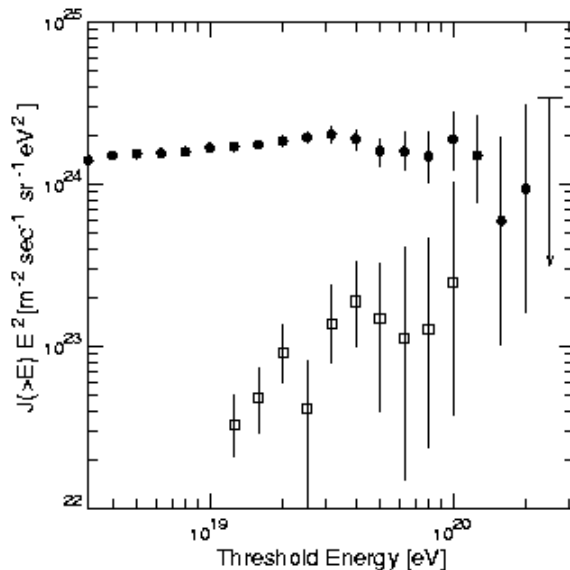


Figure 10. AGASA integrated energy spectrum of cosmic rays (closed circles) and their contribution to clustered events (open squares, see also Fig. 2). From Ref.⁶⁵.

The arrival directions of the cosmogenic neutrinos should pretty much coincide with the direction of the primary protons. Therefore, strongly interacting neutrino scenarios open a window of opportunity for the search for astrophysical point sources of post-GZK UHECR's located at cosmological distances^b. In this context, it is interesting to note that AGASA observed a clustering of events on small angular scales^{7,65,66} (cf. Fig. 2) – whose statistical significance of occurring higher than chance coincidence⁶⁷ is still being debated^{44,45,68,69}, however. Intriguingly, the integrated flux of cosmic rays contributing to the AGASA event clusters, as shown by open squares in Fig. 10, has a spectrum which is strikingly similar to the one expected from cosmogenic neutrinos in a strongly interacting neutrino scenario (cf. Fig. 7 (dashed)). Possible correlations of the arrival distributions of UHECR's with definite distant astrophysical sources such as compact radio quasars⁷⁰, in particular BL Lacertae objects⁷¹, or GRB's and magnetars⁷² may give further circumstantial evidence for an UHEC ν component in EAS data. High statistics data from forthcoming cosmic ray facilities such as Auger²² and EUSO²⁵ are required⁷³ for these investigations.

5.1.2. Searches at neutrino telescopes

The characteristic zenith angle distribution of showers in strongly interacting neutrino scenarios can of course be searched for also at neutrino telescopes where the absorbing material is, in addition to the atmosphere, the Earth as well as antarctic ice (for IceCube²³) or water (for ANTARES⁷⁴). This is illustrated in Fig. 11 (left), which displays the expected zenith angle distribution of neutrino-initiated showers above 1 EeV in a kilometer-scale detector⁵⁴. For Standard Model interactions, the distribution (solid curve) is nearly flat for down-going events, and essentially no up-going events occur due to very efficient neutrino absorption by the Earth at these energies. For models with larger cross-sections, vertical down-going events become more frequent, producing more events near $\cos\theta_{\text{zenith}} \sim 1$. At zenith angles near the horizon, $\cos\theta_{\text{zenith}} \sim 0$, more of the neutrinos are absorbed and the rate can be suppressed.

Another distinctive observable at neutrino telescopes is the energy spectrum of down-going shower events, which is shown in Fig. 11 (right) for the IceCube detector⁵⁴. The structure of this spectrum can be easily understood. As the neutrino energy exceeds the assumed threshold energy of the new interaction (cf. Fig. 6), the number of events increases dramatically above the Standard model prediction. Even farther above this energy, however, more of the neutrinos are absorbed in the ice before reaching the detector and the event rate is suppressed. This drastic “bump” structure in the spectrum indicates the sharply enhanced cross-section at the threshold. The peak of this bump occurs at the associated neutrino threshold

^bThis window of opportunity is shared with any scenario which exploits neutrinos as “messenger” particles, in particular also the Z-burst scenario.

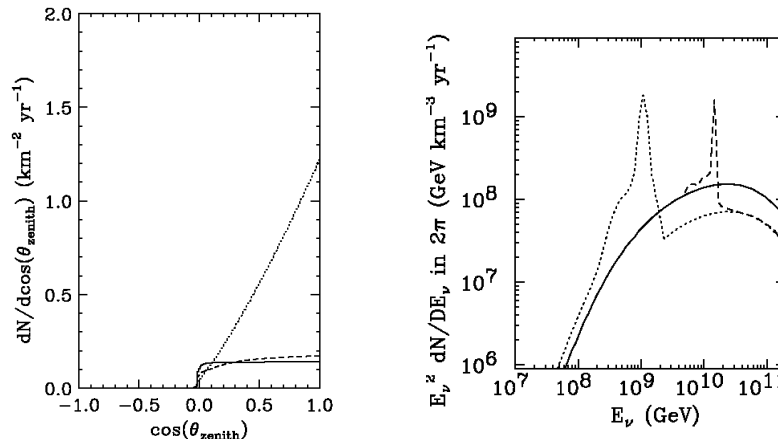


Figure 11. Characteristic observables to be studied, in the context of strongly interacting neutrino scenarios, at a kilometer-scale neutrino detector⁵⁴ such as IceCube²³. The cosmogenic neutrino flux from Ref.⁷⁵ was assumed. The dotted lines exploit the cross-section estimate from electroweak instantons from Refs.^{43,40} (cf. Fig. 6 (solid)), whereas the dashed lines represent the corresponding estimate from Refs.^{56,57} (cf. Fig. 6 (dashed)). The solid lines are the Standard Model neutral+charged current predictions.

Left: Zenith angle distribution of showers generated in neutrino-nucleon interactions. A 1 EeV energy threshold for the observed showers has been imposed.

Right: Energy distribution of down-going showers generated in neutrino-nucleon interactions.

energy and is mainly generated by charged current electron neutrino interactions. The “shoulder” slightly to the left of the bump is from neutral and charged current interactions which generate showers less energetic than the incident neutrino.

Let us mention also the possibility to look for enhanced rates for throughgoing muons (see Ref.⁷⁶ for a related study) or even spatially compact muon bundles⁴². These signatures, however, rely on details of the final state from the new interaction and are, therefore, more model-dependent than the ones discussed above, which exploit just generic shower properties.

5.2. Laboratory tests

5.2.1. (Quasi-)elastic neutrino-(electron-)nucleon scattering

As a consequence of dispersion relations, the hypothesized rapid rise in the neutrino-nucleon cross-section at large energies is felt in the elastic neutrino-nucleon scattering amplitude at much lower energies^{77c}. Exploiting unitarity and analyticity, one may relate the invariant elastic νN amplitudes $A_\pm(E)$, labeled by the nucleon

^cThis has been also pointed out in Ref.⁷⁸, however in the context of perturbative and model-dependent considerations.

helicity, with the total νN cross-section via the dispersion relation

$$\text{Re } A_{\pm}(E) - \text{Re } A_{\pm}(0) = \frac{E}{4\pi} \mathcal{P} \int_0^{\infty} dE' \left(\frac{\sigma_{\nu N}^{\text{tot}}(E', \pm)}{E'(E' - E)} + \frac{\sigma_{\bar{\nu} N}^{\text{tot}}(E', \pm)}{E'(E' + E)} \right), \quad (6)$$

where \mathcal{P} denotes the principle value of the integral. Suppose the new physics dominates the neutrino-nucleon dispersion integral (6) for $E' \geq E_{\text{th}}$ as hypothesized in a strongly interacting neutrino scenario. Assuming that $\sigma_{\nu N}^{\text{new}}$ is independent of helicity and energy, and obeys the Pomeranchuk relation $\sigma_{\nu N}^{\text{tot}}(E, \pm) - \sigma_{\bar{\nu} N}^{\text{tot}}(E, \pm) \xrightarrow{E \rightarrow \infty} 0$, a new contribution to the real part of the amplitude at energy E emerges from (6),

$$\text{Re } A_{\pm}(E) \simeq \underbrace{\text{Re } A_{\pm}(0)}_{G_F/2\sqrt{2}} + \frac{1}{2\pi} \frac{E}{E_{\text{th}}} \sigma_{\nu N}^{\text{new}}, \quad (7)$$

resulting in

$$\frac{\text{Re } A(E)_{\text{new}}}{\text{Re } A(E)_{\text{SM}}} \simeq \left(\frac{E/100 \text{ GeV}}{E_{\text{th}}/10^{18} \text{ eV}} \right) \left(\frac{\sigma_{\nu N}^{\text{new}}}{100 \text{ mb}} \right) \quad (8)$$

for the ratio of the new amplitude to the (perturbative) Standard Model (SM) amplitude. Order 100 % effects in the real elastic amplitudes begin to appear already at energies seven orders of magnitude below the full realization of the strong cross-section.

Neutrino-nucleon scattering experiments in the laboratory have therefore the opportunity to test strongly interacting neutrino scenarios by searching for enhancements in the elastic cross-sections. Current experiments at CERN and Fermilab reach energies around 100 GeV and, therefore, already start to constrain possible scenarios, e.g. p -brane production³⁷. Elastic and quasi-elastic scattering processes may be studied with the help of the H1⁷⁹ and ZEUS⁸⁰ detectors at the HERA $e^{\pm}p$ collider. Its e^{\pm} energy, in the proton's restframe, is around 10^5 GeV and, therefore, extends much beyond the energy reach of the above mentioned νN fixed-target experiments. However, one-photon exchange dominates the low-energy elastic amplitude for $e^{\pm}p \rightarrow e^{\pm}p$ to such an extent that the anomalous, new contribution is suppressed by a factor of $\sim 1/100$ compared to (8). On the other hand, possible enhancements in the quasi-elastic channels $e^+p \rightarrow \nu_e n$ and $e^-p \rightarrow \bar{\nu}_e n$, which do not suffer from QED dominance, cannot be deduced from model-independent dispersion relations. A separate calculation could be made, however, if certain aspects of the new high-energy strong-interaction are assumed.

5.2.2. Instanton searches

There is a close analogy⁸¹ between electroweak and hard QCD instanton-induced processes in deep-inelastic scattering⁸². An observably large cross-section for the latter processes at HERA is indeed necessary, but not sufficient for an observably large cross-section for the former. It seems, moreover, that a \gtrsim mb electroweak instanton cross-section necessarily requires that the bulk of inelastic small-Bjorken- x

processes is induced by soft QCD instantons, as has been proposed indeed in Ref.⁸³. Present upper limits on hard QCD instantons from the H1⁸⁴ and ZEUS⁸⁵ experiments are still above the theoretical predictions, but may be improved considerably at HERA II, within this decade. The possible direct production and observation⁸⁶ of electroweak instanton induced processes in the laboratory will have to wait for the commissioning of the VLHC⁴³.

6. Summary and conclusions

We have shown that a simple scenario with a single power-law injection spectrum of protons can describe all the features of the UHECR spectrum in the energy range $10^{17\div 21}$ eV, provided the neutrino-nucleon cross-sections becomes of hadronic size at energies above $\approx 10^{19}$ eV. In such a strongly interacting neutrino scenario, the cosmogenic neutrinos, which have been produced during proton propagation through the CMB, initiate air showers high up in the atmosphere and give thus rise to a second, neutrino-induced EAS component, extending well beyond the GZK energy. As examples giving rise to the necessary enhancement in $\sigma_{\nu N}$, we discussed p -brane production in TeV-scale gravity scenarios and Standard Model electroweak instanton-induced processes. The model for the proton injection spectrum has few parameters from which only two – the power index α and the redshift evolution index n – has a strong effect on the final shape of the spectrum. We found that, for certain values of α and n , strongly interacting neutrino scenarios are compatible with the available observational data from the AGASA and HiRes experiments (combined with their predecessor experiments, Fly’s Eye and Akeno, respectively) on the 2-sigma level (also 1-sigma for HiRes). There are a number of astrophysical source candidates, notably neutron stars and GRB’s, which may provide the necessary conditions to accelerate protons to the required energies, $E_{\max} \gtrsim 3 \times 10^{21}$ eV, by conventional shock acceleration.

The predicted ultrahigh energy cosmic neutrino component can be experimentally tested by studying the zenith angle dependence of the events in the range $10^{18\div 20}$ eV and possible correlations with distant astrophysical sources at cosmic ray facilities such as the Pierre Auger Observatory and EUSO, and by looking for bumps in neutrino-initiated shower spectra at neutrino telescopes such as ANTARES and IceCube. As laboratory tests, one may search for a enhancements in (quasi-)elastic lepton-nucleon scattering or for signatures of QCD instanton-induced processes in deep-inelastic scattering, e.g. at HERA.

In summary, strongly interacting neutrino scenarios provide a viable and attractive solution to the ultrahigh energy cosmic ray puzzle and may be subject to various crucial tests in the foreseeable future.

Acknowledgments

We would like to thank Luis Anchordoqui for valuable comments and discussions.

References

1. A. V. Olinto, in: Proc. International Workshop on *Observing Ultra High Energy Cosmic Rays from Space and on Earth*, Metepec, Puebla, Mexico, 9-12 Aug 2000, published in: AIP Conf.Proc.566:99-112,2000 [arXiv:astro-ph/0102077].
2. J. W. Cronin, S. P. Swordy and T. K. Gaisser, *Sci. Am.* **276**, 32 (1997).
3. Very Large Hadron Collider, <http://vlhc.org> .
4. Large Hadron Collider, <http://lhc-new-homepage.web.cern.ch/lhc-new-homepage> .
5. L. Anchordoqui, T. Paul, S. Reucroft and J. Swain, *Int. J. Mod. Phys. A* **18**, 2229 (2003).
6. Akeno Giant Air Shower Array, <http://www-akeno.icrr.u-tokyo.ac.jp/AGASA> .
7. M. Takeda *et al.*, *Astrophys. J.* **522**, 225 (1999).
8. K. Greisen, *Phys. Rev. Lett.* **16**, 748 (1966); G. T. Zatsepin and V. A. Kuzmin, *JETP Lett.* **4**, 78 (1966) [*Pisma Zh. Eksp. Teor. Fiz.* **4**, 114 (1966)].
9. M. Nagano *et al.*, *J. Phys. G* **18**, 423 (1992).
10. M. Takeda *et al.*, *Phys. Rev. Lett.* **81**, 1163 (1998); <http://www-akeno.icrr.u-tokyo.ac.jp/AGASA> ; date: February 24, 2003.
11. D. J. Bird *et al.*, *Phys. Rev. Lett.* **71**, 3401 (1993); D. J. Bird *et al.* [HIRES Collaboration], *Astrophys. J.* **424**, 491 (1994); D. J. Bird *et al.*, *Astrophys. J.* **441**, 144 (1995).
12. T. Abu-Zayyad *et al.* [HiRes Collaboration], astro-ph/0208243; astro-ph/0208301.
13. Z. Fodor, S. D. Katz, A. Ringwald and H. Tu, *JCAP* **0311**, 015 (2003).
14. V. L. Ginzburg and S. I. Syrovatsky, *The origin of cosmic rays*, (Pergamon Press, Oxford 1964); J. Wdowczyk and A. W. Wolfendale, *Nature* **281**, 356 (1979).
15. E. J. Ahn, G. A. Medina-Tanco, P. L. Biermann and T. Stanev, astro-ph/9911123; P. L. Biermann, E. J. Ahn, G. A. Medina-Tanco and T. Stanev, *Nucl. Phys. Proc. Suppl.* **87**, 417 (2000).
16. P. Billoir and A. Letessier-Selvon, astro-ph/0001427.
17. P. L. Biermann, E. -J. Ahn, P. P. Kronberg, G. Medina Tanco, and T. Stanev, in: *Physics and Astrophysics of Ultra-High-Energy Cosmic Rays*, eds. M. Lemoine and G. Sigl, Springer-Verlag, Berlin, 2001.
18. V. S. Beresinsky and G. T. Zatsepin, *Phys. Lett. B* **28**, 423 (1969); *Sov. J. Nucl. Phys.* **11**, 111 (1970) [*Yad. Fiz.* **11**, 200 (1970)].
19. T. J. Weiler, *Astropart. Phys.* **11**, 303 (1999); D. Fargion *et al.*, *Astrophys. J.* **517**, 725 (1999); S. Yoshida, G. Sigl and S. J. Lee, *Phys. Rev. Lett.* **81**, 5505 (1998).
20. Z. Fodor, S. D. Katz and A. Ringwald, *Phys. Rev. Lett.* **88**, 171101 (2002); *JHEP* **0206**, 046 (2002); O. E. Kalashev, V. A. Kuzmin, D. V. Semikoz and G. Sigl, *Phys. Rev. D* **65**, 103003 (2002); D. V. Semikoz and G. Sigl, hep-ph/0309328.
21. I. Kravchenko, astro-ph/0306408; P. W. Gorham, C. L. Hebert, K. M. Liewer, C. J. Naudet, D. Saltzberg and D. Williams, astro-ph/0310232; N. G. Lehtinen, P. W. Gorham, A. R. Jacobson and R. A. Roussel-Dupre, astro-ph/0309656.
22. Pierre Auger Observatory, <http://www.auger.org> .
23. IceCube, <http://icecube.wisc.edu> .
24. ANtarctic Impulse Transient Array, <http://www.ps.uci.edu/~anita> .
25. Extreme Universe Space Observatory, <http://www.euso-mission.org> .
26. Orbiting Wide-angle Light-collectors, <http://owl.gsfc.nasa.gov> .
27. Saltdome Shower Array, P. Gorham *et al.*, *Nucl. Instrum. Meth. A* **490**, 476 (2002).
28. B. Eberle, A. Ringwald, L. Song and T. J. Weiler, hep-ph/0401203.
29. F. W. Stecker, *Astrophys. J.* **228**, 919 (1979); C. T. Hill and D. N. Schramm, *Phys. Rev. D* **31**, 564 (1985); C. T. Hill, D. N. Schramm and T. P. Walker, *Phys. Rev. D* **34**,

- 1622 (1986); F. W. Stecker, C. Done, M. H. Salamon and P. Sommers, *Phys. Rev. Lett.* **66**, 2697 (1991) [Erratum-ibid. **69**, 2738 (1991)].
30. S. Yoshida and M. Teshima, *Prog. Theor. Phys.* **89**, 833 (1993).
31. R. J. Protheroe and P. A. Johnson, *Astropart. Phys.* **4**, 253 (1996); S. Yoshida, H. Y. Dai, C. C. H. Jui and P. Sommers, *Astrophys. J.* **479**, 547 (1997); R. Engel and T. Stanev, *Phys. Rev. D* **64** (2001) 093010; O. E. Kalashev, V. A. Kuzmin, D. V. Semikoz and G. Sigl, *Phys. Rev. D* **66**, 063004 (2002); Z. Fodor, S. D. Katz, A. Ringwald and H. Tu, *JCAP* **0311**, 015 (2003); D. Semikoz and G. Sigl, hep-ph/0309328.
32. J. Bordes, H. M. Chan, J. Faridani, J. Pfaudler and S. T. Tsou, hep-ph/9705463; *Astropart. Phys.* **8**, 135 (1998).
33. G. Domokos, S. Kovesi-Domokos and P. T. Mikulski, hep-ph/0006328.
34. G. Domokos and S. Kovesi-Domokos, *Phys. Rev. Lett.* **82**, 1366 (1999); S. Nussinov and R. Shrock, *Phys. Rev. D* **59**, 105002 (1999); P. Jain, D. W. McKay, S. Panda and J. P. Ralston, *Phys. Lett. B* **484**, 267 (2000); A. V. Kisselev and V. A. Petrov, hep-ph/0311356.
35. M. Kachelriess and M. Plümacher, *Phys. Rev. D* **62**, 103006 (2000); L. Anchordoqui, H. Goldberg, T. McCauley, T. Paul, S. Reucroft and J. Swain, *Phys. Rev. D* **63**, 124009 (2001).
36. E. J. Ahn, M. Cavaglia and A. V. Olinto, *Phys. Lett. B* **551**, 1 (2003); P. Jain, S. Kar, S. Panda and J. P. Ralston, *Int. J. Mod. Phys. D* **12**, 1593 (2003).
37. L. A. Anchordoqui, J. L. Feng and H. Goldberg, *Phys. Lett. B* **535**, 302 (2002).
38. G. Domokos and S. Nussinov, *Phys. Lett. B* **187**, 372 (1987).
39. S. Barshay and G. Kreyerhoff, *Eur. Phys. J. C* **23**, 191 (2002); *Phys. Lett. B* **535**, 201 (2002); S. Kovesi-Domokos and G. Domokos, hep-ph/0307098; hep-ph/0307099.
40. Z. Fodor, S. D. Katz, A. Ringwald and H. Tu, *Phys. Lett. B* **561**, 191 (2003).
41. H. Aoyama and H. Goldberg, *Phys. Lett. B* **188**, 506 (1987); A. Ringwald, *Nucl. Phys. B* **330**, 1 (1990); O. Espinosa, *Nucl. Phys. B* **343**, 310 (1990); V. V. Khoze and A. Ringwald, *Phys. Lett. B* **259**, 106 (1991).
42. D. A. Morris and R. Rosenfeld, *Phys. Rev. D* **44**, 3530 (1991); D. A. Morris and A. Ringwald, *Astropart. Phys.* **2**, 43 (1994).
43. A. Ringwald, *Phys. Lett. B* **555**, 227 (2003).
44. J. N. Bahcall and E. Waxman, *Astrophys. J.* **542**, 543 (2000).
45. Z. Fodor and S. D. Katz, *Phys. Rev. D* **63**, 023002 (2001).
46. E. Waxman, *Astrophys. J.* **452**, L1 (1995).
47. K. Hagiwara *et al.* [Particle Data Group], *Phys. Rev. D* **66**, 010001 (2002).
48. A. Mücke, R. Engel, J. P. Rachen, R. J. Protheroe and T. Stanev, *Comput. Phys. Commun.* **124**, 290 (2000).
49. Z. Fodor, S. D. Katz and A. Ringwald, in preparation.
50. X. Bertou, P. Billoir, O. Deligny, C. Lachaud and A. Letessier-Selvon, *Astropart. Phys.* **17**, 183 (2002); C. Lachaud, X. Bertou, P. Billoir, O. Deligny and A. Letessier-Selvon, *Nucl. Phys. Proc. Suppl.* **110**, 525 (2002).
51. I. Antoniadis, *Phys. Lett. B* **246**, 377 (1990); J. D. Lykken, *Phys. Rev. D* **54**, 3693 (1996); N. Arkani-Hamed, S. Dimopoulos and G. R. Dvali, *Phys. Lett. B* **429**, 263 (1998); L. Randall and R. Sundrum, *Phys. Rev. Lett.* **83**, 3370 (1999).
52. S. B. Giddings and S. Thomas, *Phys. Rev. D* **65**, 056010 (2002); S. Dimopoulos and G. Landsberg, *Phys. Rev. Lett.* **87**, 161602 (2001).
53. J. L. Feng and A. D. Shapere, *Phys. Rev. Lett.* **88**, 021303 (2002); A. Ringwald and H. Tu, *Phys. Lett. B* **525**, 135 (2002); L. A. Anchordoqui *et al.*, hep-ph/0309082.
54. T. Han and D. Hooper, *Phys. Lett. B* **582**, 21 (2004).

55. R. Gandhi, C. Quigg, M. H. Reno and I. Sarcevic, *Phys. Rev. D* **58**, 093009 (1998).
56. F. Bezrukov *et al.*, *Phys. Rev. D* **68**, 036005 (2003).
57. A. Ringwald, *JHEP* **0310**, 008 (2003).
58. M. Kachelriess, D. V. Semikoz and M. A. Tortola, *Phys. Rev. D* **68**, 043005 (2003).
59. J. N. Bahcall and E. Waxman, *Phys. Lett. B* **556**, 1 (2003).
60. D. De Marco, P. Blasi and A. V. Olinto, *Astropart. Phys.* **20**, 53 (2003).
61. A. M. Hillas, *Ann. Rev. Astron. Astrophys.* **22**, 425 (1984).
62. V. S. Berezhinsky and A. Y. Smirnov, *Phys. Lett. B* **48**, 269 (1974); C. Tyler, A. V. Olinto and G. Sigl, *Phys. Rev. D* **63**, 055001 (2001); A. Kusenko and T. J. Weiler, *Phys. Rev. Lett.* **88**, 161101 (2002).
63. R. M. Baltrusaitis *et al.*, *Phys. Rev. D* **31**, 2192 (1985).
64. S. Yoshida *et al.* [AGASA Collaboration], in: *Proc. 27th International Cosmic Ray Conference*, Hamburg, Germany, 2001, Vol. 3, p. 1142.
65. M. Takeda *et al.* [AGASA Collaboration], in: *Proc. 27th International Cosmic Ray Conference*, Hamburg, Germany, 2001, Vol. 3, p. 345.
66. M. Teshima *et al.* [AGASA Collaboration], in: *Proc. 28th International Cosmic Ray Conference*, Tsukuba, Japan, 2003, p. 437.
67. H. Goldberg and T. J. Weiler, *Phys. Rev. D* **64**, 056008 (2001).
68. S. L. Dubovsky, P. G. Tinyakov and I. I. Tkachev, *Phys. Rev. Lett.* **85**, 1154 (2000); P. G. Tinyakov and I. I. Tkachev, *JETP Lett.* **74**, 1 (2001) [*Pisma Zh. Eksp. Teor. Fiz.* **74**, 3 (2001)]; Y. Uchihori, M. Nagano, M. Takeda, M. Teshima, J. Lloyd-Evans and A. A. Watson, *Astropart. Phys.* **13**, 151 (2000); L. A. Anchordoqui, H. Goldberg, S. Reucroft, G. E. Romero, J. Swain and D. F. Torres, *Mod. Phys. Lett. A* **16**, 2033 (2001); C. B. Finley and S. Westerhoff, astro-ph/0309159.
69. C. Finley *et al.* [HiRes Collaboration], in: *Proc. 28th International Cosmic Ray Conference*, Tsukuba, Japan, 2003, p. 433.
70. G. R. Farrar and P. L. Biermann, *Phys. Rev. Lett.* **81**, 3579 (1998).
71. P. G. Tinyakov and I. I. Tkachev, *JETP Lett.* **74**, 445 (2001) [*Pisma Zh. Eksp. Teor. Fiz.* **74**, 499 (2001)]; *Astropart. Phys.* **18**, 165 (2002); D. S. Gorbunov, P. G. Tinyakov, I. I. Tkachev and S. V. Troitsky, *Astrophys. J.* **577**, L93 (2002).
72. S. Singh, C. P. Ma and J. Arons, astro-ph/0308257.
73. N. W. Evans, F. Ferrer and S. Sarkar, *Phys. Rev. D* **67**, 103005 (2003); D. F. Torres, S. Reucroft, O. Reimer and L. A. Anchordoqui, *Astrophys. J.* **595**, L13 (2003); J. Swain, astro-ph/0401632.
74. Astronomy with a Neutrino Telescope and Abyss environmental RESearch, <http://antares.in2p3.fr> .
75. R. Engel, D. Seckel and T. Stanev, *Phys. Rev. D* **64**, 093010 (2001).
76. M. Kowalski, A. Ringwald and H. Tu, *Phys. Lett. B* **529**, 1 (2002).
77. H. Goldberg and T. J. Weiler, *Phys. Rev. D* **59**, 113005 (1999).
78. G. Burdman, F. Halzen and R. Gandhi, *Phys. Lett. B* **417**, 107 (1998).
79. H1 experiment at HERA, <http://www-h1.desy.de> .
80. ZEUS experiment at HERA, <http://www-zeus.desy.de> .
81. I. I. Balitsky and V. M. Braun, *Phys. Lett. B* **314**, 237 (1993); A. Ringwald and F. Schrempp, in: *Quarks '94*, Vladimir, Russia, 1994, hep-ph/9411217.
82. S. Moch, A. Ringwald and F. Schrempp, *Nucl. Phys. B* **507**, 134 (1997); A. Ringwald and F. Schrempp, *Phys. Lett. B* **438**, 217 (1998); *Comput. Phys. Commun.* **132**, 267 (2000); *Phys. Lett. B* **503**, 331 (2001).
83. D. E. Kharzeev, Y. V. Kovchegov and E. Levin, *Nucl. Phys. A* **690**, 621 (2001); M. A. Nowak, E. V. Shuryak and I. Zahed, *Phys. Rev. D* **64**, 034008 (2001); F. Schrempp, *J. Phys. G* **28**, 915 (2002); F. Schrempp and A. Utermann, *Acta*

- Phys. Polon. B* **33**, 3633 (2002); *Phys. Lett. B* **543**, 197 (2002); hep-ph/0301177; hep-ph/0401137.
84. C. Adloff *et al.* [H1 Collaboration], *Eur. Phys. J. C* **25**, 495 (2002).
85. S. Chekanov *et al.* [ZEUS Collaboration], hep-ex/0312048.
86. G. R. Farrar and R.-B. Meng, *Phys. Rev. Lett.* **65**, 3377 (1990); A. Ringwald, F. Schrempp and C. Wetterich, *Nucl. Phys. B* **365**, 3 (1991); M. J. Gibbs, A. Ringwald, B. R. Webber and J. T. Zadrozny, *Z. Phys. C* **66**, 285 (1995); M. J. Gibbs and B. R. Webber, *Comput. Phys. Commun.* **90**, 369 (1995).